Grand-Canonical Monte Carlo Adsorption Studies on SBA-2 Periodic Mesoporous Silicas

Carlos A. Ferreiro-Rangel, Nigel A. Seaton[§], Tina Düren[†,]*

Institute for Materials and Processes, School of Engineering, The University of Edinburgh, The King's Buildings, Mayfield Road, Edinburgh EH9 3JL, UK

Current address: [§]Abertay University, Bell Street, Dundee DD1 1HG, UK

[†]Department of Chemical Engineering, University of Bath, Claverton Downs, Bath, BA2 7AY, UK

t.duren@bath.ac.uk

RECEIVED DATE (to be automatically inserted after your manuscript is accepted if required according to the journal that you are submitting your paper to)

Corresponding author contact information: Phone: +44 (0) 1225 386349

ABSTRACT

SBA-2 and STAC-1 are periodic mesoporous silicas with slightly different structures whose pore networks consist of spherical cavities interconnected by windows. This feature makes them attractive for adsorptive separation processes where the selectivity originates from molecular sieving. Recently, we were able to obtain realistic atomistic models for these materials by means of a kinetic Monte Carlo (kMC) method. In this paper, we evaluate the ability of the model to predict adsorption of both non-polar (methane and ethane) and polar (carbon dioxide) adsorptives. Predictions are in good agreement with experimental data, demonstrating the potential of these kMC-based models for use in the design of adsorption processes and the materials used in them. In particular, we show that surface roughness is a key feature for predicting adsorption in SBA-2 materials at low pressures; this is especially relevant in prospective applications such as carbon dioxide capture.

KEYWORDS

Grand Canonical Monte Carlo Simulation, Mesoporous Silicas, Adsorption, Carbon Dioxide, Ethane, Methane

Periodic mesoporous silicas (PMSs) are promising adsorbents,[1] as they offer a combination of high adsorption capacity and the scope to adjust both the size and the surface chemistry of the pores.[2] SBA-2, a PMS with spherical cavities interconnected by windows,[3-5] has been synthesized and characterized by different groups.[3-4, 6-8] Since the calcination temperature influences the size of the connecting windows, SBA-2 shows promise as an adsorbent for size- and shape-selective separations. The cavities in SBA-2 are hexagonally close-packed (hcp), reflecting the arrangement of the micelles in the precursor solution. That is, there is a sequence of two hexagonally packed layers, A and B, where the latter is slightly offset with respect to the former. A second, very similar, material is also produced as a result of this synthesis,[3] differing from SBA-2 by having cubic close packed (ccp) symmetry, characterized by an A-B-C sequence of layers. In both cases the shape and size of the pores is the same, and the material characteristically exhibits a sharp pore size distribution around the mean pore diameter.[7] Because of its different symmetry, the ccp material has a separate designation, St Andrews-Cambridge-1 (STAC-1).[3] In practice, neither material is synthesized as a pure phase, so that it is best to think of pure SBA-2 and pure STAC-1 as end-points of a spectrum of mixed materials.

Because PMSs are not crystalline, models for these materials cannot be based on knowledge of atomic coordinates from X-ray or neutron diffraction. For this reason, the first models used to represent these adsorbents were simplified, smooth-pore representations[4-5, 9-12] with surfaces that are regular at the atomic level, capturing the main structural characteristics such as pore size and shape but disregarding other important features such as the structure of the pore surface or the nature of the pore connectivity. For SBA-2, Pérez-Mendoza *et al.* proposed a model[4-5, 13] consisting of a system of smooth spheres and cylinders where the adsorption was considered to occur independently in each pore (i.e. ignoring their connections with each other) and then integrated by means of a pore size distribution (PSD). However, it is known that in reality the pore surface in PMS materials is not smooth but rather has significant

roughness[14-15] and there is a distribution of pore sizes.[7] For these reasons more realistic models are needed in order to make accurate predictions of the performance of the material in adsorption and other applications.

A different approach to modeling the structure of PMSs was taken by Schumacher and co-workers,[15-16] who developed a kinetic Monte Carlo (kMC) method that leads to atomistically realistic models of MCM-41, a PMS containing cylindrical pores. In a previous paper[17] the present authors and others extended the approach of Schumacher and co-workers to SBA-2 and STAC-1. This kMC technique mimics the key steps of the synthesis of the real materials by following the silica condensation and aggregation mechanism, according to which randomly arranged micelles accumulate layers of silica around them before spontaneously aggregating to give the long-range order of the final material.[18] A full account of this method, including the force fields used, is given in our earlier publication.[17] The model pores obtained this way show good agreement with the degree of polymerization, density, and unit-cell parameters of experimental samples. In addition, nitrogen adsorption isotherms were predicted quantitatively when compared with experimental results, which is further evidence of the realism of the kMC approach. The fact that nitrogen adsorption can be predicted accurately by single model pores generated by the kMC method, without recourse to a PSD, suggests that a substantial proportion of the heterogeneity of the real material is due to the roughness of the individual pores; however, this is not to suggest that all the pores in the corresponding real materials are of an identical size. Also, we learnt from our models that pore-connectivity in SBA-2 and STAC-1 is likely to occur through windows rather than by microporous channels,[17] as was previously assumed.[3, 5, 8, 19] (This does not imply that there are no regions of microporosity in our model, rather that the microporosity arises around the windows instead of there being distinct microporous channels.) The window-like nature of the pore connections means that adsorption takes place mainly in the spherical cavities.[17] Figure 1a shows an example of an SBA-2 simulation cell, obtained by kMC simulation; the

windows between the pores are also shown. Figure 1b shows the atomistic surface of the model pore, which arises naturally from the kMC simulation and mimics the roughness of the real materials.

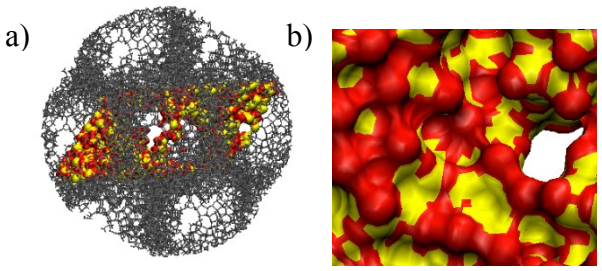

Figure 1: a) Example of a single pore in the model SBA-2 material obtained using the kMC technique. What appear to be large voids in this image are the windows connecting the cavity to its neighbors. b) Close-up of the pore surface of an SBA-2 model pore. Silicon atoms are indicated in yellow, and oxygen atoms in red. Hydrogen atoms are omitted for clarity.

In this work, we investigate the ability of our kMC-based model material to predict adsorption. This analysis, which involves a combination of Monte Carlo simulation of adsorption and experimental adsorption measurements, is of interest for two reasons. Firstly, adsorption allows us to further investigate the realism of the model material, which is of fundamental interest in the study of the synthesis and structure of SBA-2. Adsorption at low pressure is very sensitive to surface roughness and (for polar adsorptives) to surface polarity, while adsorption at high pressure explores pore size and pore geometry. Secondly, we evaluate the applicability of the model materials to adsorption technology; if it can be demonstrated that the adsorption of a range of gases can be reliably predicted, these models can be applied to the design of gas storage and separation processes, and to the tailoring of PMS-based adsorbents for use in such applications. To this end, we use these kMC-generated model pores to study the adsorption of non-polar (CH_4 and C_2H_6) and polar (CO_2) fluids on SBA-2/STAC-1, exploring the predictive capability of these models for adsorptives with different properties.

We also investigate the adsorbent force-field for these materials, and in particular the question of the transferability of parameters – an issue that is critical to the prediction of adsorption using molecular simulation. The Lennard-Jones potential-well depth parameter for the silanol oxygens, $(\varepsilon_o/k_B)_{solid}$, commonly used for simulating adsorption in PMSs is 185 K,[4-5, 9, 15-16, 20] but this parameters was obtained by studying ethane adsorption on a smooth-pore representation of MCM-41,[9] while our SBA-2 model pores exhibit realistic pore roughness. For this reason, we study its transferability to our model pores, acknowledging that, along with surface roughness, $(\varepsilon_o/k_B)_{solid}$ has a great impact on adsorption at low pressure. The simulated adsorption isotherms are compared to experimental results obtained by Pérez-Mendoza and co-workers[4-5] on a sample calcined at 550 °C.

SIMULATION METHOD

The kMC simulation method is presented in full in our earlier paper.[17] Here we focus on aspects that are relevant to the modeling of adsorption in the model materials and the comparison of the adsorption predictions with experimental data. As we indicated earlier, the real material is in practice a mixture of SBA-2 (with hcp symmetry) and STAC-1 (with ccp symmetry).[3] In order to obtain the hcp symmetry of SBA-2, the simulation cell must contain two cavities while for the ccp symmetry of STAC-1 a single cavity is sufficient.[17] Henceforth we refer to the "single-cavity" model as SC, and TC for the "two-cavity" model, both representative of the distinct phases in the mixed material produced experimentally. We compare our simulated adsorption results with experimental data reported by Pérez-Mendoza,[4-5] who estimated a pore size of ~47 Å for the experimental material sample.

Table 1 summarizes the main characteristics of the model pores used for this study. The diameter of each of the cavities, the variation of the local pore surface from a spherical shape (expressed as a standard deviation), and the connections of the cavities via the windows to their neighbors were studied by means of the random walk technique described elsewhere.[17] The accessible surface area of these

materials was determined by simulating rolling a probe molecule across the surface.[21] In both these computations, a probe with a diameter of 3.3 Å was used.

The SC model pore used for this study has a mean cavity diameter of 47.2 Å and standard deviation of 3.7 Å, while the two pores in the TC model have mean cavity diameters of 47.6 and 48.9 Å with standard deviations of 1.8 Å and 2.5 Å, respectively. (The fact that the two pores in the TC model have different structural properties is simply a consequence of the stochastic nature of the kMC simulation.) The higher standard deviation of the SC model is already an indication of its higher surface roughness when compared to the TC pore model. The pores in the SC and TC models have a similar surface area.

Table 1: Properties of the SC and TC models used in this study.

	SC	**TC**
Unit cell parameter (Å)	52.1 / 53.3 / 50.1	53.2 / 53.2 / 85.5
Unit cell mass (g/mol)	5.17×10^4	1.09×10^5
Number of Si atoms	810	1693
Number of silanol oxygen atoms	341	797
Pore diameter (Å)	47.2 (±3.7)	47.6 (±1.8) / 48.9 (±2.5)
Surface area (m^2/g)	1290	1245
Skeletal density (g/cm^3)	3.31	3.29

Adsorption was simulated using grand canonical Monte Carlo (GCMC) simulation.[22] In this method, the thermodynamic state is defined by constant temperature T, constant volume V, and constant chemical potential for each adsorptive species i, μ_i, which was related to the pressure using the Peng-Robinson equation of state, with parameters matched to experimental fluid properties.[23-24] We modeled Coulombic interactions using the Ewald summation technique[22] and dispersive interactions using the 12-6 Lennard-Jones (LJ) potential, with the Lorentz-Berthelot mixing rules being used to calculate mixed Lennard-Jones parameters. The LJ parameters and partial charges used in this work are given in Table 2.

Table 2: Interaction parameters used in the GCMC adsorption simulations.

	Site	ε_i/k_B (K)	σ_i (Å)	q_i (e_o)	Reference
Pore wall	Si	165-200§	0.0	1.2805	9, 15-16
	bO		2.708	-0.6402	
	nbO		3.000	-0.5261	
	H		0.0	+0.2060	
He	He	10.90	2.640	-	25
CH_4	CH_4	147.90	3.730	0.0	26
C_2H_6 *	CH_3	139.80	3.775	0.0	26
CO_2 **	C	29.00	2.79	0.66450	27
	O	82.00	3.06	-0.33225	

* The CH_3-CH_3 bond length in ethane molecules is 1.53 Å

** The C-O bond length in CO_2 molecules is 1.161 Å

§ Range of values studied in this work

A value of 185 K for the LJ potential-well depth of the oxygen atoms in the adsorbent is widely used in the literature for simulating adsorption in PMSs,[4-5, 9, 15-16, 20] particularly in the case of MCM-41. However, this parameter was originally derived for MCM-41 using experimental data for the adsorption

of ethane and model pores with smooth walls.[9] Unlike in the MCM-41 model originally used to set the value of the LJ potential-well depth, the kMC-generated pores are rough, and spherical in shape rather than cylindrical. It is thus likely that the appropriate LJ potential-well depth will be different for the model pores studied here, since the oxygen-adsorptive potential would be expected to more closely reflect the true interatomic interactions, without having also to compensate for an unrealistically smooth surface. This would be in line with recent simulation results for neopentane adsorption in kMC-generated MCM-41pores, which showed this value had to be changed to get good agreement between simulation and experiment.[20]

GCMC simulations give the absolute amount adsorbed, N_{abs}, as a function of pressure. Experimentally, however, the excess amount adsorbed, N_{ex}, is measured. The transformation from one to the other is done through[9, 25]

$$N_{ex} = N_{abs} - \rho_{bulk} V_{He} \quad \textbf{(1)}$$

where V_{He} is the pore volume, which is obtained by the GCMC simulation of helium adsorption (mimicking the use of helium to measure the pore volume in adsorption experiments), and ρ_{bulk} is the density of the bulk adsorptive at the simulated temperature and pressure, which is calculated using the Peng-Robinson equation of state.

The isotherms predicted by our models are scaled by the ratio of the maximum amount adsorbed measured experimentally and that predicted by simulating adsorption in the model pores, thus accounting for the difference in pore size between the model pores and the pores in the experimental sample (since they are not an exact match), and also for any non-porous defects such as pore blocking that are present on real samples but are not accounted for in the pore models.

First we determined the optimal value of $(\varepsilon_o/k_B)_{solid}$ for predicting adsorption in the SC model by using a non-polar adsorptive, ethane, and assigning different values of this parameter for the oxygen atoms in the pore wall. We used the experimental ethane isotherm at 273 K, a relatively low temperature, because the location of the point of inflection, which is a sensitive measure of the strength of the solid-fluid interaction, becomes more prominent as the temperature is reduced. We studied values of $(\varepsilon_o/k_B)_{solid}$ from 135 K to 200 K.

Figure 2 shows the predicted ethane isotherms using three different values for $(\varepsilon_o/k_B)_{solid}$ compared with the experimental SBA-2 isotherm measured by Pérez-Mendoza *et al.*[4-5] Using 185 K, the value widely used for MCM-41 simulations, as the potential well depth in the SC model leads to slight overpredictions of ethane uptake in the low-pressure range, suggesting that this value is too high. Thus, in Figure 2 we also present isotherms for $(\varepsilon_o/k_B)_{solid}$ equal to 165 K and 135 K.

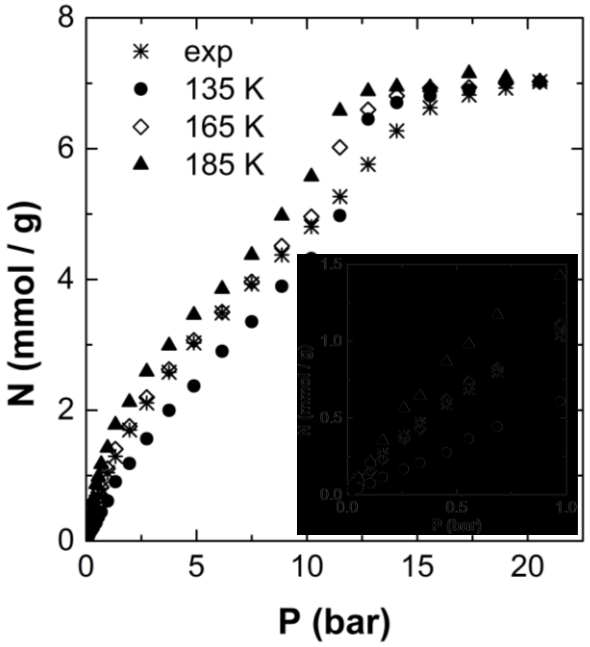

Figure 2: Experimental and simulated ethane adsorption isotherms at 273 K for different values of $(\varepsilon_o/k_B)_{solid}$ in the SC model. The inset shows the low pressure region of the adsorption isotherms.

A reduction in $(\varepsilon_o/k_B)_{solid}$ to 165 K improves the overall isotherm prediction including the low pressure region of the isotherm, which is a very sensitive measure for the fluid-solid interaction, while a further reduction to $(\varepsilon_o/k_B)_{solid}$ = 135 K gives much poorer results. This suggests that the optimal value is in the region of 165 K; this is confirmed by the calculation of the mean-squared errors in predicting the experimental isotherm, shown in Figure 3.

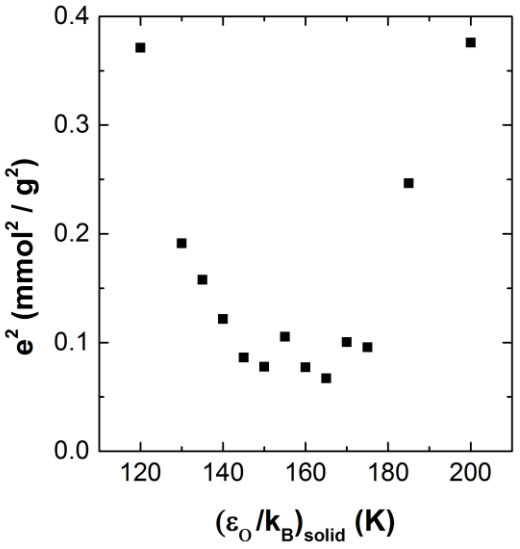

Figure 3: Mean-squared error for the deviation of the predicted ethane isotherms from the experimentally measured isotherm as a function of $(\varepsilon_o/k_B)_{solid}$.

The observation that decreasing the value of the LJ parameter ε from the one originally derived for atomistically smooth model pores of MCM-41[9] leads to overall improvement in adsorption predictions reflects the fact that the rough surface of our model pores results in a stronger overall solid-fluid interaction than would exist with a smooth surface. It is worth noting that, even with the optimal value of $(\varepsilon_o/k_B)_{solid}$, pore filling in the model pores consistently occurs at P ~ 12 bar, slightly lower than

the value measured experimentally. This indicates that the size of the model pore is somewhat smaller than that of the experimental sample.

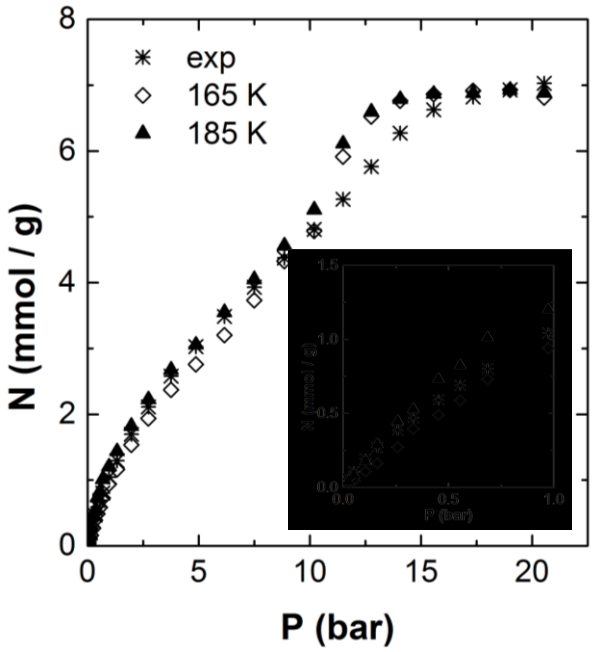

Figure 4: Ethane isotherms at 273 K predicted with the TC model for two values of $(\varepsilon_o/k_B)_{solid}$. The inset shows the low pressure region of the adsorption isotherms.

To further investigate the role of the LJ parameter $(\varepsilon_o/k_B)_{solid}$, in Figure 4 we present the predicted ethane isotherms at 273 K, now using the TC model. As in the SC model, there is good agreement in the low pressure region between the simulated and experimental adsorption isotherms. The pore filling pressure (the pressure at the point of inflection of the isotherm) is slightly underestimated, and whilst the difference between using the potential well depth for the adsorbent as 185 K or 165 K is not as marked as in the case of the SC model it can still be seen that the latter provides a better overall approximation to the experimental isotherm. We hypothesize that, since the pores in both the SC and TC models have comparable sizes, this is due to the smoother pore surfaces in the TC model pores (as indicated by the smaller standard deviations in the pore diameters reported in Table 1), resulting in an

effective decrease in the solid-fluid interaction. (This difference in roughness reflects the structure of these particular realizations of the SC and TC model pores, and should not be interpreted as reflecting a difference in the average roughness of pores arranged according to different symmetries.)

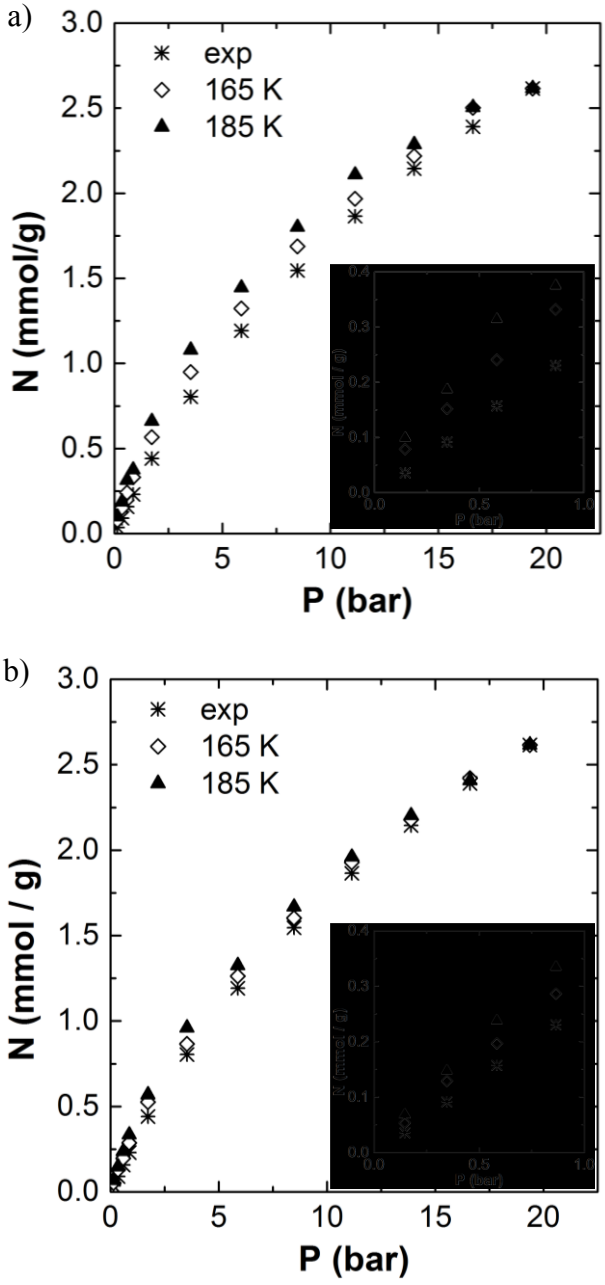

Figure 5: Methane isotherms at 263 K for two values of $(\varepsilon_o/k_B)_{solid}$ using a) the SC model and b) the TC model. The insets show the low pressure regions of the adsorption isotherms.

Given the overall improved adsorption predictions by the newly proposed value for the LJ parameter, we now use this new value in simulating the adsorption of other species. Since the SBA-2 experimental sample is not phase-pure, Figure 5shows methane adsorption predictions at 263 K using both the SC (Figure 5 a) and TC (Figure 5 b) models. While both predicted isotherms are very close to the experimental results over the whole pressure range, the better match is obtained with the TC model. The new value of 165 K leads to better predictions in the low pressure range thus providing further evidence that for both pore models the new Lennard-Jones parameter gives a better representation of the solid-fluid interactions than the commonly used value of 185 K, supporting the transferability of this parameter. [To be clear, by "transferability" we mean in this context the applicability of a fixed parameter value to different model materials of the same general class – in this case, models for PMS materials generated by kMC simulation. Of course, this is not to say that the same parameter value should be used for a smooth-pore model of the same PMS.] These results could be further improved by lowering $(\varepsilon_o/k_B)_{solid}$ further, but this would compromise the prediction at higher pressures. Since the shape of the cavities in both the SC and the TC models is the same and methane adsorption in neither model material reaches pore filling, the difference in the predicted adsorption isotherm must be due to differences in the fluid-wall interactions, which in turn reflects the degree of surface roughness on the model pores. The fact that the predicted adsorption at low pressure is lower in the TC model than in the SC model again points to the surface of the TC model being less rough. The interaction of the methane molecules with the pore surface is illustrated in Figure 6, which shows that the small methane molecules can reside within nooks in the pore wall that are just big enough for them to enter; these are not accessible to larger molecules such as ethane.

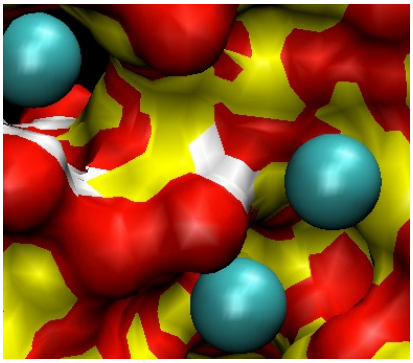

Figure 6: Snapshot showing methane molecules trapped in nooks in the surface of the SC model pore. Color code: yellow- Si atoms; red- oxygen atoms; white- hydrogen atoms; and blue- methane molecules.

Having studied systems with non-polar adsorptives, we now look at the predictive performance of the models when the adsorptive is polar in nature and both dispersive and electrostatic interactions play an important role. Figure 7 presents carbon dioxide predictions for both $(\varepsilon_o/k_B)_{solid}$ parameters at 263 K in the SC and TC model pores.

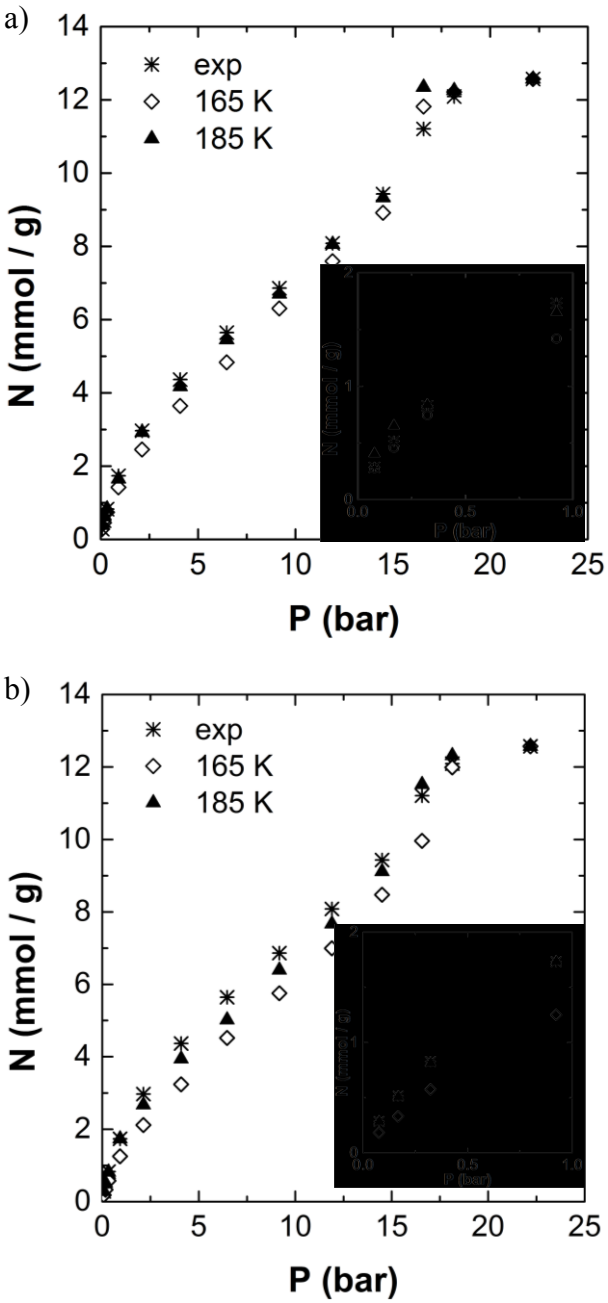

Figure 7: CO_2 isotherms at 263 K for two values of $(\varepsilon_o/k_B)_{solid}$ using a) the SC model and b) the TC model. The insets show the low pressure regions of the adsorption isotherms.

As illustrated in Figure 7a, the use of $(\varepsilon_o/k_B)_{solid}$ = 165 K for CO_2 in the SC pore model shows no improvement in the low pressure region predictions as well as a more marked inflection in the isotherm. The mean-squared error for the deviation between simulated and experimental isotherm is 0.0271

$mmol^2$ / g^2 for $(\varepsilon_o/k_B)_{solid}$ = 165 K and 0.0099 $mmol^2$ / g^2 for $(\varepsilon_o/k_B)_{solid}$ = 185 K. Also, as expected, the value of $(\varepsilon_o/k_B)_{solid}$ has little impact on the accuracy of the predictions at higher pressures. Note that the SC model gives better predictions for CO_2 than it did for ethane, including better prediction of the pore-filling pressure.

Figure 7b shows CO_2 adsorption predictions using the TC model. As in the case of the SC model, the general features of the CO_2 isotherm are realistically captured, whilst quantitatively the simulations slightly underpredicted the experimental adsorption. When using the TC model, contrary to what was seen with the SC model, predictions at low pressure obtained using $(\varepsilon_o/k_B)_{solid}$ = 185 K are slightly more accurate. As in the case of ethane adsorption, this reflects the fact that the TC model has cavities with smoother pore surfaces than those of the SC model, and the larger $(\varepsilon_o/k_B)_{solid}$ parameter for the solid compensates for the lower solid-fluid interactions.

CONCLUSIONS

We used models of SBA-2/STAC-1 generated by kMC simulation to study the adsorption of species of differing molecular size and polarity. The agreement between simulated and experimental adsorption isotherms is very good, particularly for ethane and CO_2. Methane adsorption is slightly overestimated, perhaps because the simulated material has pore surfaces that are slightly rougher than the real material. The fact that there are generally accurate predictions over the entire pressure range for both polar and non-polar adsorptives is a good indication that these model pores are a realistic representation of SBA-2/STAC-1 from the point of view of adsorption. As adsorption is a sensitive probe of both surface structure and pore geometry, our results strongly support the realism of kMC-generated models for these materials, and suggest their wider applicability to PMSs. These models

provide a useful tool for predicting the impact of material properties on adsorption in this class of materials, and for designing new PMS-based adsorbents for applications in gas storage and separation.

The Lennard-Jones potential-well depth parameter $(\varepsilon_o/k_B)_{solid}$ commonly used for predicting adsorption in MCM-41 is found to overpredict adsorption at low pressures in SBA-2/STAC-1, and upon optimization a value of 165 K, in general, was found to provide better results (though for the TC model, adsorption of CO_2 at low pressure is better predicted by $(\varepsilon_o/k_B)_{solid}$ = 185 K). The better predictive behavior of the model pores with $(\varepsilon_o/k_B)_{solid}$ = 165 K seems to be due to the more realistic, rough nature of the pore surface, in contrast to the simplified, smooth surface of the models used to determine the literature value of $(\varepsilon_o/k_B)_{solid}$ = 185 K. This emphasizes that care must be taken when transferring parameters between models representing different systems, where the models have been generated using different methodologies.

ACKNOWLEDGEMENTS

We thank the European Commission (EU FP6 STREP SES6CT2005-020133 "DeSANNS") and The University of Edinburgh for financial support, as well as Dr. Christian Schumacher and Dr. Manuel Pérez-Mendoza for their helpful advice. This work has made use of the resources provided by the Edinburgh Computer and Data Facility (ECDF). (http://www.ecdf.ed.ac.uk/). The ECDF is partially supported by the eDIKT initiative (http://www.edikt.org.uk)

REFERENCES

1. Rouquerol, F.; Rouquerol, J.; Sing, K., *Adsorption by Powder & Porous Solid*. Academic Press: London, 1999.
2. Huo, Q. S.; Margolese, D. I.; Ciesla, U.; Feng, P. Y.; Gier, T. E.; Sieger, P.; Leon, R.; Petroff, P. M.; Schüth, F.; Stucky, G. D., Generalized Synthesis of Periodic Surfactant Inorganic Composite-Materials. *Nature* **1994,** *368*, 317-321.

3. Zhou, W. Z.; Hunter, H. M. A.; Wright, P. A.; Ge, Q. F.; Thomas, J. M., Imaging the Pore Structure and Polytypic Intergrowths in Mesoporous Silica. *J. Phys. Chem. B* **1998,** *102*, 6933-6936.
4. Perez-Mendoza, M.; Gonzalez, J.; Wright, P. A.; Seaton, N. A., Elucidation of the Pore Structure of SBA-2 using Monte Carlo Simulation to Interpret Experimental Data for the Adsorption of Light Hydrocarbons. *Langmuir* **2004,** *20*, 7653-7658.
5. Perez-Mendoza, M.; Gonzalez, J.; Wright, P. A.; Seaton, N. A., Structure of the Mesoporous Silica SBA-2, Determined by a Percolation Analysis of Adsorption. *Langmuir* **2004,** *20*, 9856-9860.
6. Huo, Q. S.; Leon, R.; Petroff, P. M.; Stucky, G. D., Mesostructure Design with Gemini Surfactants - Supercage Formation in a 3-Dimensional Hexagonal Array. *Science* **1995,** *268*, 1324-1327.
7. Kim, J. M.; Stucky, G. D., Synthesis of Highly Ordered Mesoporous Silica Materials Using Sodium Silicate and Amphiphilic Block Copolymers. *Chem. Comm.* **2000**, 1159-1160.
8. Hunter, H. M.; Wright, P. A., Synthesis and Characterisation of the Mesoporous Silicate SBA-2 and its Performance as an Acid Catalyst. *Microporous Mesoporous Mater.* **2001,** *43*, 361-373.
9. Yun, J.-H.; Düren, T.; Keil, F. J.; Seaton, N. A., Adsorption of Methane, Ethane, and Their Binary Mixtures on MCM-41: Experimental Evaluation of Methods for the Prediction of Adsorption Equilibrium. *Langmuir* **2002,** *18*, 2693-2701.
10. Maddox, M. W.; Olivier, J. P.; Gubbins, K. E., Characterization of MCM-41 Using Molecular Simulation: Heterogeneity Effects. *Langmuir* **1997,** *13*, 1737-1745.
11. Maddox, M. W.; Sowers, S. L.; Gubbins, K. E., Molecular Simulation of Binary Mixture Adsorption in Buckytubes and MCM-41. *Adsorption* **1996,** *2*, 23-32.
12. Sliwinska-Bartkowiak, M.; Dudziak, G.; Sikorski, R.; Gras, R.; Radhakrishnan, R.; Gubbins, K. E., Melting/Freezing Behavior of a Fluid Confined in Porous Glasses and MCM-41: Dielectric Spectroscopy and Molecular Simulation. *J. Chem. Phys.* **2001,** *114*, 950-962.
13. Perez-Mendoza, M.; Gonzalez, J.; Ferreiro-Rangel, C. A.; Lozinska, M. M.; Fairen-Jimenez, D.; Düren, T.; Wright, P. A.; Seaton, N. A., Pore-Network Connectivity and Molecular Sieving of Normal and Isoalkanes in the Mesoporous Silica SBA-2. *J. Phys. Chem. C* **2014,** *118*, 10183-10190.
14. Coasne, B.; Hung, F. R.; Pellenq, R. J. M.; Siperstein, F. R.; Gubbins, K. E., Adsorption of Sample Gases in MCM-41 Materials: The Role of Surface Roughness. *Langmuir* **2006,** *2*, 194-202.
15. Schumacher, C.; Gonzalez, J.; Wright, P. A.; Seaton, N. A., Generation of Atomistic Models of Periodic Mesoporous Silica by Kinetic Monte Carlo Simulation of the Synthesis of the Material. *J. Phys. Chem. B* **2006,** *110*, 319-333.
16. Schumacher, C.; Gonzalez, J.; Perez-Mendoza, M.; Wright, P. A.; Seaton, N. A., Design of Hybrid Organic/Inorganic Adsorbents Based on Periodic Mesoporous Silica. *Ind. Eng. Chem. Res.* **2006,** *45*, 5586-5597.
17. Ferreiro-Rangel, C. A.; Lozinska, M. M.; Wright, P. A.; Seaton, N. A.; Düren, T., Kinetic Monte Carlo Simulation of the Synthesis of Periodic Mesoporous Silicas SBA-2 and STAC-1: Generation of Realistic Atomistic Models. *J. Phys. Chem. C* **2012,** *116*, 20966-20974.
18. Corma, A., From Microporous to Mesoporous Molecular Sieve Materials and their Use in Catalysis. *Chem. Rev.* **1997,** *97*, 2373-2419.
19. Hunter, H. M.; Garcia-Bennett, A. E.; Shannon, I. J.; Zhou, W. Z.; Wright, P. A., Particle Morphology and Microstructure in the Mesoporous Silicate SBA-2. *J. Mater. Chem.* **2002,** *12*, 20-23.
20. Herdes, C.; Ferreiro-Rangel, C. A.; Düren, T., Predicting Neopentane Isosteric Enthalpy of Adsorption at Zero Coverage in MCM-41. *Langmuir* **2011,** *27*, 6738-6743.
21. Düren, T.; Millange, F.; Férey, G.; Walton, K. S.; Snurr, R. Q., Calculating Geometric Surface Areas as a Characterization Tool for Metal−Organic Frameworks. *J. Phys. Chem. C* **2007,** *111*, 15350-15356.
22. Frenkel, D.; Smit, B., *Understanding Molecular Simulation, Second Edition: From Algorithms to Applications (Computational Science Series, Vol 1)*. Academic Press: 2001.
23. Hill, T. L., *Statistical Mechanics: Principles and Selected Applications*. 1st ed.; McGraw-Hill: USA, 1956.

24. van Wylen, G. J.; Sonntag, R. E., *Fundamentals of Classical Thermodynamics*. 3rd ed.; John Wiley & Sons Inc.: 1986.
25. Talu, O.; Myers, A. L., Molecular Simulation of Adsorption: Gibbs Dividing Surface and Comparison with Experiment. *AIChE J.* **2001,** *47*, 1160-1168.
26. Jorgensen, W. L.; Maxwell, D. S.; TiradoRives, J., Development and Testing of the OPLS All-Atom Force Field on Conformational Energetics and Properties of Organic Liquids. *J. Am. Chem. Soc.* **1996,** *118*, 11225-11236.
27. Harris, J. G.; Yung, K. H., Carbon Dioxide's Liquid-Vapor Coexistence Curve And Critical Properties as Predicted by a Simple Molecular Model. *J. Phys. Chem.* **1995,** *99*, 12021-12024.

TOC: